Pergamon

Bioorganic & Medicinal Chemistry 9 (2001) 2501–2510

BIOORGANIC & MEDICINAL CHEMISTRY

Nucleic Acid Triggered Catalytic Drug and Probe Release: A New Concept for the Design of Chemotherapeutic and Diagnostic Agents

Zhaochun Ma and John-Stephen Taylor*

Department of Chemistry, Campus Box 1134, Washington University, One Brookings Drive, St. Louis, MO 63130, USA

Received 2 February 2001; accepted 5 July 2001

Abstract—Recently, we described a new concept for the design of highly selective antiviral and anticancer chemotherapeutic agents that makes use of a disease-specific nucleic acid sequence to template the association of a prodrug with a catalyst which catalyzes the release of the drug. Herein, we report on the effect of mismatches, sterics, and electronics on the rate and specificity of drug and probe release in both two and three component model systems, and on the stability of the prodrug linker in human serum.

Introduction

The goal of chemotherapy is to design or discover drugs that are selectively toxic to the diseased cell or the disease causing organism.[1,2] This is a quite difficult challenge for cancer chemotherapy, however, because there is often little, biochemically, to distinguish a normal cell from a cancerous cell. Most chemotherapeutic drugs found by traditional screening approaches have been found to interfere with replication and cell division and owe their selectivity to the fact that cancer cells divide more rapidly than normal cells. Unfortunately, the chemotherapeutic indices for these drugs are often quite low. More recently, new approaches to chemotherapy have sought to take advantage of what has been learned about the biochemistry of cancer cells to design more effective drugs.[3–5] Promising as these approaches are, individual drugs would have to be developed for each type of cancer, and would still be susceptible to drug resistance through mutations in the target enzymes or proteins that are acquired by the rapidly dividing cancer cells.

Another approach to obtaining highly selectively chemotherapeutic agents is to further increase the selectivity of known agents by selectively targeting prodrugs, or prodrug metabolizing enzymes to diseased cells.[4–12] Most notable among such approaches is ADEPT (antibody directed enzyme prodrug therapy), in which an antibody that recognizes a disease-specific antigen is linked to a prodrug metabolizing enzyme which leads to the release of a cytotoxic agent outside the cell. A related approach involves targeting of a gene coding for a prodrug metabolizing enzyme (GDEPT) by either chemical or viral methods to activate the prodrug within the cell. Unfortunately, the success of these types of approaches also depends on the existence of significant biochemical differences between normal and diseased cells that can be used for targeting, and would likewise be susceptible to drug resistance.

An ideal type of prodrug chemotherapy would involve activation of the prodrug specifically within the diseased cell without the need for targeting, and without the need to know the biochemical basis of the disease. It is with these criteria in mind that we have recently proposed a new and general concept for the design of easily programmable and highly selective chemotherapeutic drugs that we have termed nucleic acid triggered catalytic drug release.[13] Our basic idea is to convert a disease-specific nucleic acid sequence into a prodrug metabolizing catalyst specifically within a diseased cell by way of the high specificity and simplicity of Watson–Crick base pairing. In one embodiment of this idea (Fig. 1), the prodrug metabolizing catalyst is created by a catalytic component consisting of a catalytic group attached to an oligonucleotide analogue which binds tightly and specifically to a unique site on a disease-specific nucleic

*Corresponding author. Tel.: +1-314-935-6721; fax: +1-314-935-4481; e-mail: taylor@wuchem.wustl.edu

0968-0896/01/$ - see front matter
PII: S0968-0896(01)00245-0

acid sequence, such as a unique or overexpressed mRNA sequence. The prodrug in turn consists of a cytotoxic drug that is attached via a cleavable linker to an oligonucleotide analogue that binds reversibly to the site adjacent to the catalytic component binding site. When the catalytic component binds to the disease-specific nucleic acid sequence, a prodrug metabolizing enzyme-like species is created which contains both a prodrug binding site and a catalytic site. This enzyme-like catalyst then catalyzes multiple releases of a cytotoxic drug from the prodrug. In a normal cell, the disease-specific nucleic acid sequence is either absent, or in low copy number, and the drug will be inefficiently released. The beauty of this approach, if it could be realized, is that one only needs to be able to identify the unique or over expressed nucleic acid sequences that are unique to the diseased cell and not their biological function, something which can now be readily determined by DNA chip technology.[14,15] In the event of a mutation in the triggering sequence, it would be quite simple to synthesize a new complementary pair of prodrug and catalytic components. In the event of acquired resistance to the effects of the cytotoxic drug used, a different drug could be readily attached to the prodrug component.

We have recently validated this new approach to programmable chemotherapeutic agents with an in vitro three component system based on the imidazole catalyzed hydrolysis of *p*-nitrophenyl esters.[13] In that study, we showed that *p*-nitrophenol could be released catalytically and with turnover from a prodrug component consisting of a D-valine-*p*-nitrophenylester linked octamer ODN and a catalytic component consisting of an imidazole linked 15-mer ODN in the presence of a 23-mer triggering ODN. Herein, we will describe some further studies of this three component system, as well as studies of a simpler hairpin model system, in an effort to better understand the effects of mismatches, sterics, and electronics on the rate and specificity of drug release. We will also report on the effect of sterics and electronics on the stability of the aryl ester subunit of the prodrug component in human serum.

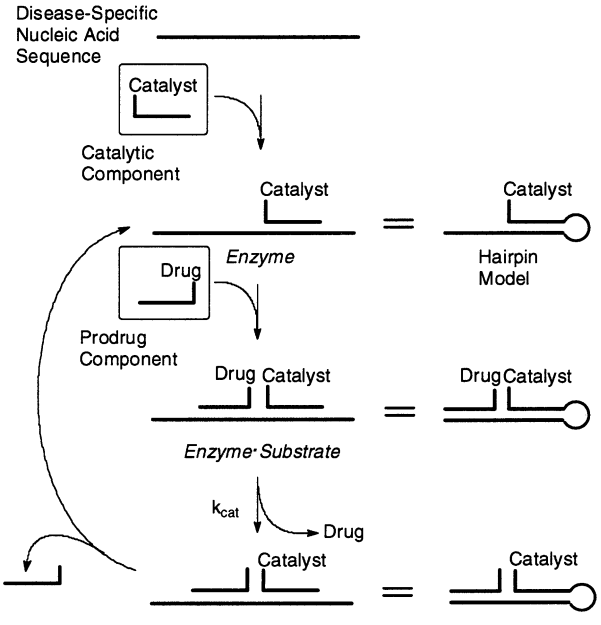

Figure 1. Nucleic acid triggered catalytic drug release. The idea is to convert a disease specific nucleic acid sequence into a drug releasing enzyme-like catalyst by complex formation with a complementary catalyst-bearing nucleic acid or analogue. To the right is a simpler two-component model system that can be used to evaluate the catalytic efficiency of various catalyst drug combinations.

Results and Discussion

Hairpin model system

When we originally began our studies of this new approach to chemotherapeutic agents, we made use of a simpler two component model system in which the catalytic component was directly fused to the triggering nucleic acid sequence via a hairpin loop (Fig. 1). This was done so as not to complicate the interpretation of the kinetics by reversible binding of the catalytic component to the triggering nucleic acid, and to insure a stoichiometric association between the catalytic component and the triggering component. A d(CTTG) tetraloop flanked by dG and dC was chosen for the hairpin loop based on a previous study which showed this type of sequence to form a very stable hairpin structure when fused to a five base-pair stem.[16] The catalytic group was chosen to be imidazole because it is well known to catalyze the hydrolysis of *p*-nitrophenylesters[17–19] as well as other arylesters.[20] In addition, release of a phenol is the key step in the release of cytotoxic drugs such as daunorubicin, phenol mustards, and fluorouracil from hydroxymethylphenyl-based prodrugs,[21–23] and taxol from trimethylene lock-based prodrugs[24] (Fig. 2). The imidazole was attached to the hairpin by a previously described procedure[25] involving coupling of the thiobenzylester phosphoramidite building block **1** to CPG-supported ODN in the last synthesis cycle to give the intermediate thiobenzylester **2** followed by treatment with excess histamine to give **3a** (Fig. 3). Temperature dependent UV absorbance spectroscopy demonstrates

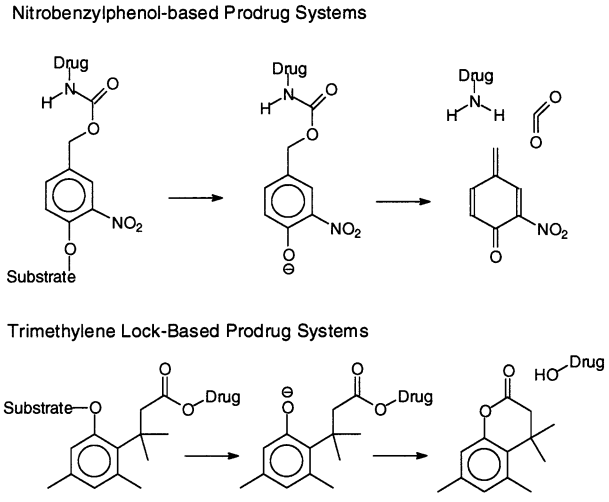

Figure 2. Prodrugs whose activation is triggered by the initial release of a phenol group.

that the hairpin **3a** is indeed stable at room temperature, and has a T_M of 65 °C in 0.1 M NaCl, and 75 °C in 1 M NaCl. This compares favorably with the calculated values of 60 and 71 °C, respectively,[26] and a T_M of 71 °C at 1 M NaCl reported for d(GGAGCTTGCTCC).[16]

Fluorescein diester hairpin system

Because of the strong fluorescence and widespread use of fluorescein as a fluorescent probe, we had first decided to investigate the rate of fluorescein release by imidazole catalyzed hydrolysis of diacetyl fluorescein. Diacetylated fluoresceins are non fluorescent, but upon hydrolysis of the acyl groups become highly fluorescent. Attempts to attach the *N*-hydroxysuccinimide derivative of diacetylcarboxyfluorescein via amide bond formation with the 3′-amino linked oligodeoxynucleotide **5** (Fig. 4) failed due to the high pH required for the reaction which led to the premature hydrolysis of the acetate groups. Attempts to conjugate 5-chloromethyl fluorescein diacetate with a 3′-phosphorothioate labeled ODN also failed at pH 7. Coupling could be achieved, however, with the more base stable pivaloyl derivative **6** by a procedure that has previously been used to link it to 5′-amino linked oligodeoxynucleotide analogues.[27] Three ODNs **7a–c**, corresponding to a 4-mer, 6-mer and 8-mer were derivatized with bis-pivaloyl fluorescein to test the effect of ODN length on the efficiency of hydrolysis by the imidazole hairpin **3a**. The T_Ms of **7a–c** were estimated from thermodynamic parameters to be −20, 19, and 41 °C under the conditions of the experiment and have equilibrium dissociation constants of 3.4 mM, 8.1 μM, and 14 nM.[28]

As expected, the rate of fluorescein release was greatest for the 8-mer **7c** and roughly corresponded to the rate of release observed in 0.01 mM imidazole buffer alone at pH 7 (Fig. 5). The relative initial rates of fluorescein release for **7a–c** under otherwise identical conditions were 1:48:493. The observed relative rates are similar to those of 1:188:340 that would be predicted based on the initial rate being proportional to $(K_d + [S])^{-1}$ if the system is following a Michaelis–Menten mechanism (vide infra), given that the concentration of imidazole hairpin enzyme and substrate are the same. In addition, it is assumed that k_{cat} will be the same for all three substrates. Attempts, however, to fit the rate of fluorescein release from **7a–c** in the presence of **3a** to Michaelis–Menten kinetics, or the rate of fluorescein release from fluorescein dipivalate by imidazole to a one or two step mechanism were not successful.

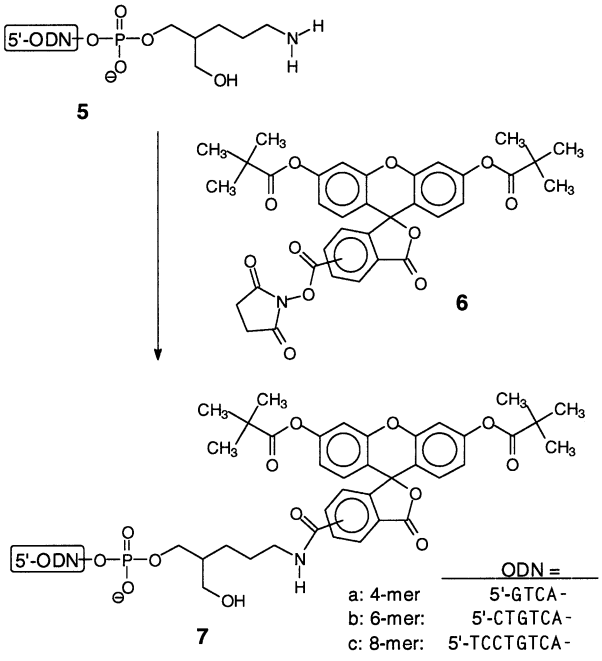

Figure 4. Synthesis of the fluorescein dipivalate proprobes.

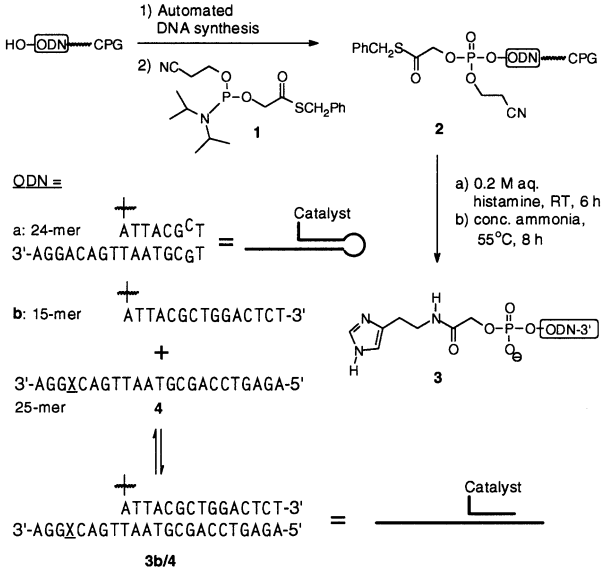

Figure 3. Synthetic scheme for the preparation of the hairpin enzyme for the two-component model system and the catalytic component for the three component system.

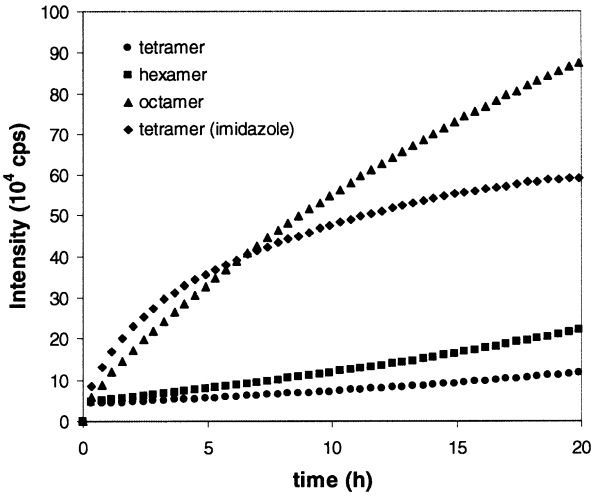

Figure 5. Effect of oligodeoxynucleotide length on the activation of the fluorescein dipivalate ODNs (10 μM) by the imidazole hairpin **3a** (5 μM) in 0.1 M phosphate buffer (pH 7.0) at 20 °C with excitation at 490 nm and detection at 525 nm. For comparison, the release of fluorescein from the fluorescein tetramer **7a** by imidazole at 0.01 M imidazole alone is also shown.

β-Alanine-nitrophenol hairpin system

To get more interpretable kinetic data, we shifted our studies to monitoring *p*-nitrophenolate release. Because of the greater sensitivity of *p*-nitrophenyl esters to hydrolysis by base than the pivalate esters, we discovered that we could not use the pH 9 conditions that had worked successfully for coupling of the pivalate esters by amide bond formation. Unfortunately, the yields of amide bond formation at neutral pH by a variety of methods were very poor and we had to change the coupling strategy. One recently reported method for coupling peptides to ODNs under neutral conditions involves addition of a thiol derivatized ODN to a maleimide derivatized peptide.[29] To this end we prepared a maleimide linked *p*-nitrophenyl ester **9** (Fig. 6) by condensing β-alanine with maleic anhydride to form the maleamic acid derivative **8** which was then refluxed with thionyl chloride followed by addition of *p*-nitrophenol according to a general procedure.[30] The resulting maleimide *p*-nitrophenyl ester **9** was then linked to an ODN 8-mer by reduction of the disulfide protected ODN **14** that was prepared by automated synthesis utilizing a commercially available support.

When the prodrug **15a** was incubated with the imidazole hairpin **3a**, catalytic release of *p*-nitrophenolate was observed that depended on the presence of the imidazole group (Fig. 7). As one can see, the half life for release of a single *p*-nitrophenolate is only about 10 min, and four turnovers are complete in about 4 h. We found that the initial rate of *p*-nitrophenolate release followed simple Michaelis–Menten kinetics,[31] and was subject to competitive inhibition by the disulfide linked oligodeoxynucleotide **14** (Fig. 8). The experimental K_I and K_M values of 38 and 50 μM (Table 2) are more than 3 orders of magnitude higher than the expected value of 14 nM for the dissociation constant K_d of the prodrug and inhibitor based on available thermodynamic parameters.[28] One possibility for the large difference between K_M and the calculated K_d values is that k_{cat} is much greater than k_{off}.[31] Given that the on rate for duplex formation is weakly temperature and sequence dependent and within an order of magnitude of $10^6\ M^{-1}\ s^{-1}$ for many oligodeoxynucleotides,[32] the sum of k_{off} and k_{cat} would have to be about $50\ s^{-1}$ to account for the observed K_M. Given that the experimentally determined k_{cat} value is $2.9\times10^{-3}\ s^{-1}$, k_{off} would have to be $50\ s^{-1}$. Thus, it would appear that $k_{off} \gg k_{cat}$ and that *p*-nitrophenolate release is governed by a Michaelis–Menten mechanism in which K_M essentially equals K_d.

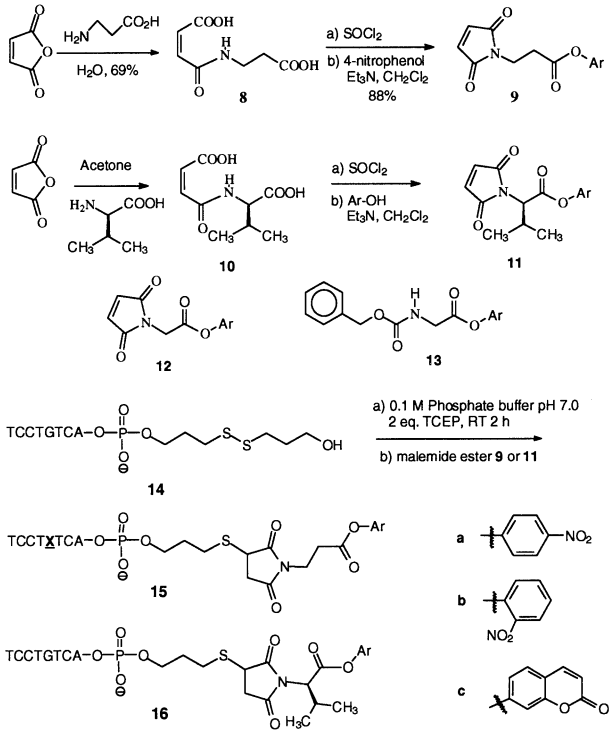

Figure 6. Synthesis of the *p*-nitrophenol-based prodrugs and hydroxycourmarin-based proprobes.

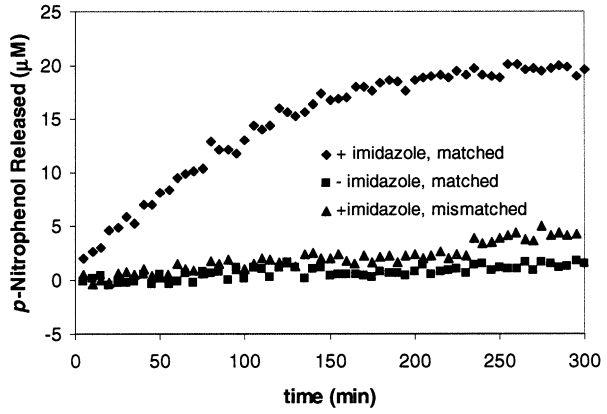

Figure 7. Kinetics of *p*-nitrophenolate release from 20 μM of the matched β-alanine 8-mer prodrug **15a** (X = G) in the presence of 5 μM of the imidazole hairpin **3a** (+imidazole, matched) or the hairpin lacking the imidazole group (−imidazole, matched) in 10 mM phosphate, 1 M NaCl, pH 7, at 20 °C. Also shown are the kinetics of *p*-nitrophenolate release from the mismatched prodrug component **15a** (X = C) in the presence of the imidazole hairpin **3a** (+imidazole, mismatched).

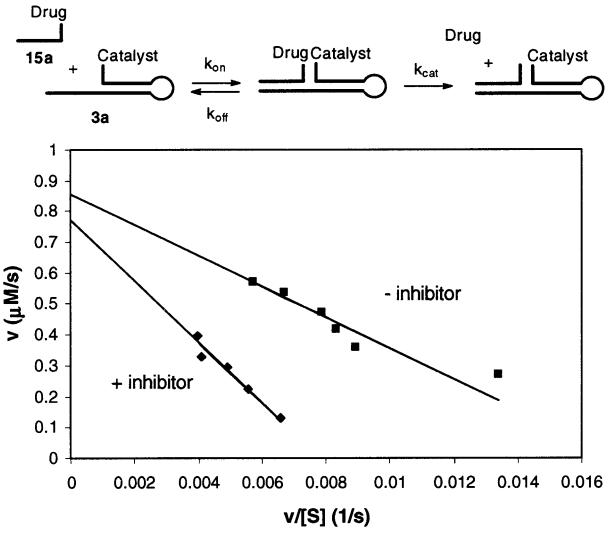

Figure 8. Eadie–Hofstee plots of the kinetic data for *p*-nitrophenolate release from the matched β-alanine 8-mer prodrug **15a** (X = G) by the imidazole hairpin in the presence and absence of the 8-mer inhibitor **14**.

The substantially higher K_I and K_M values than predicted is somewhat perplexing, and might be due to destabilizing steric and electrostatic interactions caused by close proximity of the functional groups appended to the 5′- and 3′-ends of the ODNs through phosphodiester linkages. It would not appear that much of the destabilization is due to electrostatics, as only a modest increase in K_M from 50 to 80 μM was observed on decreasing the salt concentration from 1 M NaCl to 0.1 M (Table 1). The difference between K_M and the calculated K_d might also be due to the inaccuracy in using thermodynamic parameters obtained close to the T_M to predict equilibrium constants at temperatures much different than the T_M value.[33]

The imidazole hairpin system was found to enhance the rate of ester hydrolysis 446-fold relative to imidazole by comparing the bimolecular rate constant given by k_{cat}/K_M to the bimolecular rate constant for imidazole-catalyzed hydrolysis of *p*-nitrophenylacetate, k_{Im} (Table 2). We also found that that there was an 11-fold difference in the initial rates of *p*-nitrophenolate release at 1 M NaCl between the completely complementary substrate-hairpin **3a·15a** (X=G) and a single CC base-pair mismatch resulting from a G→C transversion in the substrate component **15a** (X=C) (Fig. 7). Assuming that the rates are proportional to $(K_d+[S])^{-1}$ for the reasons cited above, the observed 11-fold rate difference would have to be accounted for by a 15-fold increase in the K_d of the mismatch substrate. This is more than 3 orders of magnitude less than that calculated from standard thermodynamic parameters which predict a 5×10^4 difference in K_d for the corresponding unmodified ODNs.[28,34] A similar insensitivity to a mismatch was also observed in our previous study of a three component system involving a D-valine ester linkage and a TC mismatch in place of TA.[13] In that case only a 1.4-fold difference in rate was observed in 1 M NaCl, which could be increased to a 7.5-fold difference in 0.1 M salt. Again, these unexpectedly low differences in rates between matched and mismatched substrates might result from unfavorable interactions between the ends of the hairpin and substrate, as well as the inaccuracy of predicting free energy differences at temperatures remote from the T_M.[33]

D-Valine-*p*-nitrophenol hairpin system

To be effective as a prodrug, the chemical linkage between the nucleic acid and the drug must be labile to the catalytic component but at the same time be stable to endogenous enzymes. To increase the stability of the ester linkage between the nucleic acid and the drug activating component we decided to examine the effect of substituting the β-alanine linkage with the sterically more demanding D-valine linkage. Unnatural D-amino acid esters have been shown to decrease the rate of ester hydrolysis by esterases, proteases and lipases.[35–38] The D-valine linkage could be introduced by the same methodology used for incorporating the β-alanine ester, as we have recently reported.[13] When the D-valine ester **16a** was used in place of the β-alanine ester **15a** with the imidazole hairpin **3a**, the rate of *p*-nitrophenolate release dropped significantly. Analysis of the kinetic data by Michaelis–Menten kinetics showed that the loss could be attributed primarily to a 8.3-fold drop in k_{cat} (Table 1). Such a drop in the rate constant is consistent with what has been previously observed to occur to the rate of imidazole catalyzed hydrolysis of *p*-nitrophenylacetate upon alkyl substitution.[39] When compared to the rate of hydrolysis by imidazole alone (Table 2), the imidazole hairpin was found to accelerate the rate of hydrolysis of the β-alanine and D-valine *p*-nitrophenyl-esters to the same extent (446 versus 429, respectively) as calculated by $(k_{cat}/K_M)/k_{Im}$ (Table 1).

Table 1. Kinetic parameters for two component system consisting of the 8-mer prodrugs **15a** (X = G), **16a**, or **16c** and the hairpin enzyme **3a** at 20 °C, in 10 mM phosphate buffer pH 7.0

	β-Alanine-*p*-nitrophenyl ester **15a** (X = G) 1.0 M NaCl	β-alanine-*p*-nitrophenyl ester **15a** (X = G) 0.1 M NaCl	D-Valine-*p*-nitrophenyl ester **16a** 1.0 M NaCl	D-Valine hydroxy coumarin ester **16c** 1.0 M NaCl
V_{max} (μM/s)	$1.4\pm0.1\times10^{-2}$	$1.5\pm0.1\times10^{-2}$	$1.7\pm0.2\times10^{-3}$	$2.22\pm0.05\times10^{-4}$
K_m (μM)	50±7	82±15	57±13	16±1
k_{cat} (s^{-1})	$2.9\pm0.2\times10^{-3}$	$3.0\pm0.2\times10^{-3}$	$3.5\pm0.4\times10^{-4}$	$4.4\pm0.1\times10^{-5}$
K_I (μM)	38±3	nd	nd	nd
k_{Im}($M^{-1}\cdot s^{-1}$)	$1.3^a\times10^{-1}$	$1.3^a\times10^{-1}$	$1.43\pm0.04\times10^{-2}$	$1.13\pm0.07\times10^{-3}$
Enhancement	446	281	429	2433

[a]For *p*-nitrophenylacetate.

Table 2. Kinetic parameters for the imidazole catalyzed hydrolysis of *p*-nitrophenyl and 3-hydroxycoumarin esters at pH 7 in 0.5 M NaCl at 20 °C, where k_o is the background hydrolysis rate constant, and k_{Im} is the imidazole catalyzed rate constant

Ester	k_o (s^{-1})	k_{Im} ($M^{-1}\,s^{-1}$)
p-Nitrophenylacetate	4.4×10^{-5}	0.13
Mal-D-valine-*p*-nitrophenylacetate, **11a**	$4.1\pm2\times10^{-6}$	$1.4\pm0.04\times10^{-2}$
Mal-D-glycine-coumarin, **12c**	$1.3\pm6\times10^{-4}$	$7.9\pm0.1\times10^{-2}$
Mal-β-alanine-coumarin, **9c**	$2.1\pm2\times10^{-5}$	$5.7\pm0.05\times10^{-2}$
Mal-D-valine-coumarin, **11c**	$4.9\pm4\times10^{-7}$	$1.13\pm0.07\times10^{-3}$
CBZ-glycine-coumarin, **13c**	$1.0\pm5\times10^{-4}$	$9.2\pm0.5\times10^{-2}$

D-Valine-7-hydroxycoumarin ester hairpin system

Whereas the *p*-nitrophenolate may be a suitable system for drug release, it is not very suitable for diagnostic purposes because of the low sensitivity of absorbance spectroscopy used to detect *p*-nitrophenolate release. We therefore decided to examine the ability of our imidazole based system to release the well known fluorescent probe 7-hydroxycoumarin otherwise known as umbelliferone.[40] Hydroxycoumarin was linked to the 8-mer through a D-valine linkage to give **16c** in the same way used to link the *p*-nitrophenol (Fig. 6). When incubated with the imidazole hairpin **3a**, release of the hydroxycoumarin was found to be about 10-fold slower than for *p*-nitrophenol. Analysis of the kinetics by Michaelis–Menten kinetics established that k_{cat} was about 10-fold lower than for *p*-nitrophenol release, and that K_M was also lower (Table 1). The 10-fold decrease in k_{cat} was also observed for k_{Im} (Table 2) and is consistent with the higher pK_a of 7-hydroxycoumarin than *p*-nitrophenol (7.8 versus 7.15) and the known effect of increasing pK_a of the phenol group on decreasing the rate of imidazole catalyzed hydrolysis.[18,20] The lower K_M for hydroxycoumarin release may be due to additional stability imparted by intercalation of the coumarin into the DNA, though this difference in K_M is not apparent for the three component system to be discussed later. When compared to hydrolysis by imidazole alone, a 2433-fold rate acceleration was calculated (Table 1) which is greater than the rate acceleration of 1100 observed for hydrolysis of a related hydroxycoumarin by a semisynthetic catalytic antibody.[41]

D-Valine-7-hydroxycoumarin 3-component system

Having established that the imidazole hairpin could catalyze the release of both *p*-nitrophenol and hydroxycoumarin that were linked to an 8-mer substrate, we investigated the ability of the three component system to release hydroxycoumarin. We have previously reported on the kinetics of the three component D-valine-linked *p*-nitrophenol system[13] in which the imidazole hairpin component is replaced by a imidazole 15-mer **3b** which binds to a complementary 23-mer **4** (X = A) that corresponds to a disease-specific triggering sequence. In this case, the complex formed between the catalytic component **3b** and the triggering ODN **4** (X = A) was designed to be highly stable and to function as an enzyme. This is justified considering the predicted kinetics of dissociation of the complex. The 15-mer was calculated to have a K_d's at 20 °C of 4.3 fM and 0.012 fM in 0.1 and 1 M NaCl,[28] respectively, and duplex half lives of much greater than a year based on an on rate of $10^6\,M^{-1}\,s^{-1}$.[32] As was the case for the three component *p*-nitrophenol system, release of hydroxycoumarin followed Michaelis–Menten kinetics. As we had observed for the imidazole hairpin system, replacing *p*-nitrophenol with coumarin in the three component system resulted in about a 10-fold decrease in rate that could be attributed to a 10-fold drop in k_{cat} (Table 3). Likewise, the kinetic parameters for both the hairpin and three component systems were also found to be quite similar.

Stability of the maleimide esters in human serum

To determine whether or not prodrugs or proprobes based on the D-valine ester linkages would be suitable for use in humans we investigated the stability of the maleimide esters of *o*-nitrophenol and 3-hydroxycoumarin **D-11b** and **D-11c** in human serum. We found that these two esters are hydrolyzed at a significant rate at 25 °C with a half life of about 3 h (Fig. 9). Interestingly, the two rates appear to be similar, suggesting that the rate determining step for hydrolysis in serum may not be the initial release of the *p*-nitrophenol or the hydroxy coumarin, but may instead be the hydrolysis of a rapidly formed acyl enzyme intermediate. We also compared the stability of the D-valine esters to the maleoyl-β-alanine, maleoyl-glycine and CBZ-glycine coumarin esters, **9c**, **12c** and **13c**, and the L-valine ester **L-11c**. We found that the maleoyl-β-alanine and maleoyl-glycine esters were more stable than the CBZ-glycine ester, but much less stable than the maleoyl-D-valine esters to hydrolysis by human serum. Presumably, the maleoyl group makes these derivatives poorer substrates for the enzymes involved in the hydrolysis reaction, as there is not a substantial difference in reactivity between these substrates with respect to imidazole catalyzed hydrolysis (Table 2). The stereochemistry at the α-carbon also plays a role, as the D-valine esters are more slowly hydrolyzed by about of factor of about two than the L-valine ester **L-11c**.

Implications of the kinetics for drug or probe selectivity in vivo

There would appear to be two parameters of importance in determining the maximum degree of selectivity achievable from the nucleic acid triggered drug and probe release system described. The first is the number of copies of the triggering nucleic acid in the diseased cell relative to the normal cell, and the second is whether or not the prodrug binding site on the triggering nucleic acid differs in sequence, and hence K_M between the normal and diseased cells. From a simple consideration of the Michaelis–Menten mechanism and the results of this study the relative rates would appear to be given by:

$$\frac{v_{diseased}}{v_{normal}} = \frac{[NA]_{diseased}(K_d + [prodrug])_{normal}}{[NA]_{normal}(K_d + [prodrug])_{diseased}}$$

Table 3. Kinetic parameters for three component system consisting of the 8-mer prodrug **16a** or proprobe **16c**, 15-mer catalytic component **3b**, and 23-mer template **4** (X = A) in 10 mM sodium phosphate buffer, pH 7.0 at 20 °C

	D-Valine-nitrophenylester **16a**[a] 1.0 M NaCl	D-Valine-coumarin ester **16c** 1.0 M NaCl
V_{max} (μM/s)	$1.5 \pm 0.02 \times 10^{-3}$	$1.54 \pm 0.04 \times 10^{-4}$
K_m (μM)	22 ± 1.2	18 ± 1
k_{cat} (s^{-1})	$3.0 \pm 0.04 \times 10^{-4}$	$3.08 \pm 0.08 \times 10^{-5}$
K_I (μM)	$1.7 \pm$	9 ± 1
k_{Im} (M^{-1}/s)	$1.4 \pm 0.04 \times 10^{-2}$	$1.13 \pm 0.07 \times 10^{-3}$
Enhancement	974	1514

[a]From Ma and Taylor.[13]

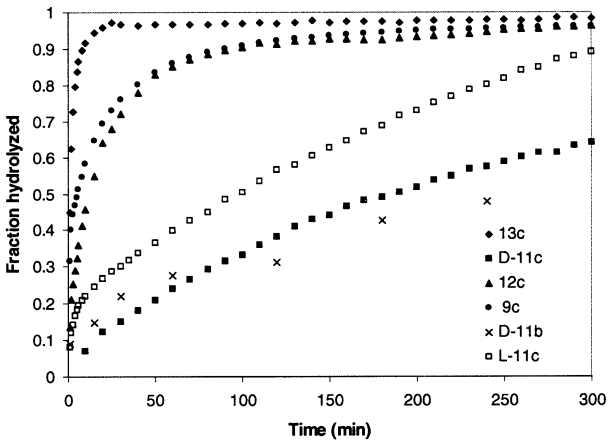

Figure 9. Stability of various esters that could be used as prodrug linkers in human serum at 20 °C temperature at pH 8.3.

where [NA] represents the concentration of the nucleic acid trigger, K_d is the dissociation constant for the drug component binding to the triggering sequence, [prodrug] is the concentration of the prodrug. In deriving this equation, the assumption is made that enough catalytic component is present with a high enough binding constant to saturate the nucleic acid trigger and hence the enzyme concentration would equal the concentration of the nucleic acid trigger. The second assumption is that, independent of any specific targeting system, the concentration of drug component would be the same in all cells. A third assumption is that k_{cat} will be the same for any catalytic complex that assembles in either the normal or the diseased cells. Thus, selective drug release could be achieved by either or both the presence of an overexpressed triggering sequence, such as an overexpressed mRNA sequence, or by having the prodrug binding site differ in sequence, and hence K_M. For the latter two cases, it is clear from the derived expression for selectivity, that it would be important to have $K_d \gg$[prodrug] to achieve maximum selectivity.

Another important consideration in designing the nucleic acid catalyzed prodrug releasing components is that they are only activated by the disease-specific nucleic acid sequence, and that drug release is efficient. In humans, a minimum sequence length of 15–17 nucleotides has been suggested to be required to uniquely recognize a specific RNA transcript. In our system, the required specificity is embedded within the catalytic component, which by design is composed of a long sequence to anchor it to the RNA. Also, as part of the design, the prodrug component must have a sufficient off rate to allow for turnover. If the length of the sequence is too short and hence not specific, the rate of drug release could be inhibited by non-productive binding of the prodrug component to other accessible sites. Thus it would also be important to design a sequence of sufficient length to insure specificity of prodrug binding, and of sufficiently low binding affinity to insure that it would have a fast enough off rate to allow for rapid turnover. If necessary, low binding affinity could be engineered into the sequence by use of an affinity lowering backbone analogue, or appropriate substituents.

Conclusion

We have begun to get a better understanding of the scope and limitations of the imidazole-based nucleic acid triggered catalytic drug and probe releasing system and have found that the rate of their release is sensitive to both steric and electronic effects. We have also found that the K_ms are higher and mismatch discrimination lower than expected from standard thermodynamic parameters, which may have to do with the nature of the linkers used to tether the catalysts and probes to the oligodeoxynucleotides. It still remains to be determined whether the imidazole system can be made to be suitable for in vivo drug or probe release purposes, as even the D-valine esters of the *o*-nitrophenyl and 7-hydroxycoumarin esters are hydrolyzed at a significant rate within human plasma. To work well, the prodrug and proprobe components will have to be much more resistant to hydrolysis by endogenous enzymes but not to the drug releasing catalyst. Unfortunately, we found that increased substitution of the ester linkage causes a decrease in the rate of imidazole catalyzed hydrolysis as does an increase in the pK_a of the displaced phenol. Nonetheless, if nucleic acid triggered catalytic drug release could be realized in vivo, it would be superior to other approaches because it would only depend on the presence of a disease specific nucleic acid sequence and not on a biochemical targeting or activating mechanism. The additional beauty of this system would appear to be the potential to use thermodynamic parameters to optimize the sequence of the prodrug component and hence the selectivity for a specific triggering sequence, and thus the ability to tailor a drug system for an individual patient.

Experimental

Materials and methods

Dichloromethane and triethylamine were dried by refluxing with CaH_2 overnight followed by distillation. Benzyl mercaptan, dimethylaminopyridine (DMAP), 1,3-dicyclohexylcarbodiimide (DCC), dichloroacetic acid, 2-(cyanoethyl)-*N*,*N*,*N*′,*N*′-tetraisopropylphosphorodiamidite, histamine, maleic anhydride, thionyl chloride and β-alanine were purchased from Aldrich (Milwaukee, WI). Tris(2-carboxyethyl)phosphine hydrochloride (TCEP·HCl) was purchased from Pierce (Rockford, IL). Reagents for automatic oligonucleotides synthesis were purchased from Glen Research (Sterling, VA). Oligonucleotides were assembled on an Applied Biosystems 380 DNA synthesizer using phosphoramidite chemistry and recommended protocols (DMTr off synthesis). Oligonucleotides were purified by reversed phase HPLC as described below in detail. ^{1}H NMR, ^{13}C NMR and ^{31}P NMR spectra were obtained on either a Varian UnityPlus-300 (300 MHz) or Varian Mercury-300 (300 MHz) spectrometer. The chemical shifts are expressed in ppm downfield from residual chloroform ($\delta = 7.24$) and acetone ($\delta = 2.04$) as an internal standard. ^{31}P NMR spectra were referenced against 85% H_3PO_4 in a coaxial insert. Flash chromatography was performed

on Selecto Scientific silica gel. Thin layer chromatography (TLC) was run on pre-coated 254 nm fluorescent silica gel sheets manufactured by Alltech (Dearfield, IL). UV spectral data were acquired on a Bausch and Lomb Spectronic 1001 spectrophotometer or Varian Cary 1E UV–vis Spectrophotometer. Fluorescence measurements were carried out on a SPEX Fluoromax instrument. MALDI mass spectra of oligodeoxynucleotides were measured on PerSeptive Voyager RP MALDI-TOF mass spectrometer.

Synthesis of the imidazole hairpin (3a). The oligonucleotides were assembled on commercial nucleoside derivatized columns using standard protocols. Phosphoramidite[1] (reference) was used in the last coupling step (0.1 M in acetonitrile; 30 min coupling time). After oxidation with 0.1 M iodine, the protected ODN **2a** was treated with 0.2 M histamine in water for 6 h. 1 Complete deprotection was carried out in concentrated aqueous ammonia at 55 °C for 8 h. The ammonia solution was evaporated to dryness on a Savant Speedvac, first under water aspirator pressure and then under high vacuum to yield the crude oligomer **3a**. It was then dissolved in doubly distilled water and purified by reversed phase HPLC on a Rainin Dynamax column (C-18, 5 μm, 4.6×250 mm) using two buffers: A [100 mM triethyl ammonium acetate buffer pH 7.0(50%)/water (50%)] and B [100 mM triethyl ammonium acetate buffer pH 7.0 (50%)/acetonitrile (50%)]. A linear gradient was run from 0 to 30% B in 30 min, flow rate = 1.0 mL/min. The wavelength of the detector was set at 260 nm. The pure fraction was collected, concentrated and desalted by using the same column, washed with excess doubly distilled water and eluted with 50:50 acetonitrile/water. The desalted fractions were combined and concentrated to dryness in vacuo. The product **3a** was analyzed by MALDI-TOF, calcd ($M-H^+$) 7622.0, found 7621.3.

Synthesis of fluorescein dipivalate oligodeoxynucleotide conjugates (7). To a mixture of DMF (32 μL) and 0.1 M $NaHCO_3/Na_2CO_3$ buffer (pH 9) (140 μL) were added successively a solution of 3′-amino-linked oligo **5** (1.2 mM in water, 36 nmol) and a solution of the activated ester **6** (12 mM in DMF, 1.44 μmol). The turbid mixture was stirred vigorously at room temperature for 1.5 h in the dark. The oligodeoxynucleotide conjugates **7** were purified by preparative reverse-phased HPLC on a Ranin Dynamax column (solvent A = 0.05 M triethylammonium acetate, pH 7; solvent B = 80% acetonitrile in buffer A; linear gradient, from 7 to 63% of B over 20 min and then to 100% of B over 20 min; flow rate = 1 mL min^{-1}). Yield (measured by UV absorbance at 260 nm) was 25% after purification. The conjugates were analyzed by MALDI-MS *m/z* [M−H] **7a**: calcd 1910.5, obsd 1909.2; **7b**: calcd 2503.9, obsd 2502.5; **7c**: calcd 3097.3, obsd 3095.8.

Synthesis of the maleamic acid of β-alanine (8). β-Alanine (8.9 g, 100 mmol) was dissolved in 10 mL of water. Maleic anhydride (9.8 g, 100 mmol) was added all at once and the mixture was stirred for 4 h at ambient temperature. After completion of the reaction, the mixture was filtered and the white power obtained was washed with water (3×10 mL) followed by anhydrous ethanol (3×10 mL), and then anhydrous ether (3×10 mL). After drying, 11.6 g (69%) of the maleamic acid was obtained. ^{1}H NMR (300 MHz, D_2O) δ 2.45 (t, J = 6.4 Hz, 2H), 3.32 (t, J = 6.4 Hz, 2H), 6.06 (d, J = 12.4 Hz, 1H), 6.26 (d, J = 12.4 Hz, 1H); HRMS(FAB) calcd for $C_7H_{10}NO_5$ ($M+H^+$) 188.0559, found 188.0558.

Synthesis of *N*-maleoyl-β-alanine-4-nitrophenol ester (9a). The maleic acid **6** was dissolved in 20 mL of thionyl chloride and heated at reflux until gas evolution had ceased. The excess thionyl chloride was evaporated under reduced pressure. Carbon tetrachloride was added to the remaining material, and the resulting solution was evaporated under reduced pressure to insure complete removal of thionyl chloride. The resulting product was dissolved in 20 mL of CH_2Cl_2 and was slowly added to a stirred mixture of 4-nitrophenol (0.82 g, 5.9 mmol) and triethylamine (1.6 mL, 12 mmol) in 20 mL of CH_2Cl_2 at 0 °C. The reaction mixture was allowed to warm to room temperature. After stirring an additional half hour at room temperature, the reaction mixture was diluted with 200 mL CH_2Cl_2, washed with brine, water, dried over Na_2SO_4 and concentrated in vacuo. The residue was recrystallized in ethyl acetate and hexane mixture (v/v = 1:1) to afford the ester **9a**, 1.5 g (88%). ^{1}H NMR (300 MHz, $CDCl_3$) δ 2.92 (t, J = 6.9 Hz, 2H), 3.98 (t, J = 6.9 Hz, 2 H), 6.74 (s, 2H), 7.30 (d, J = 9.0 Hz, 2H), 8.26 (d, J = 9.0 Hz, 2H); ^{13}C NMR (300 MHz, $CDCl_3$) δ 33.3, 33.4, 122.5, 125.2, 134.3, 145.4, 155.0, 168.4, 170.2; HRMS calcd for $C_{13}H_{10}N_2O_6Na$ ($M+Na^+$) 313.0436, found 313.0439.

Synthesis of *N*-maleoyl-β-alanine-coumarin ester (9c). The maleamic acid of β-alanine **8** (475 mg, 2.54 mmol) was dissolved in 6 mL of thionyl chloride and heated at reflux until gas evolution had ceased. The excess thionyl chloride was evaporated under reduced pressure. Carbon tetrachloride was added to the remaining material, and the resulting solution was evaporated under reduced pressure to ensure complete removal of thionyl chloride. The resulting product was dissolved in 10 mL of THF and was slowly added to a stirred mixture of 7-hydroxycoumarin (411 mg, 2.54 mmol) and triethylamine (0.74 mL, 5.36 mmol) in 20 mL of THF at 0 °C. The reaction mixture was allowed to warm to room temperature. After stirring an additional half hour at room temperature, the reaction mixture was diluted with 200 mL ethyl acetate, washed with brine, water, dried over Na_2SO_4 and concentrated in vacuo. The residue was flash chromatographed on silica gel (1:1 ethyl acetate/hexane) to afford the *N*-maleoyl-β-alanine ester **9c**, 300 mg (38%). ^{1}H NMR (300 MHz, $CDCl_3$) δ 2.92 (t, J = 6.6 Hz, 2H), 3.97 (t, J = 6.8 Hz, 2H), 6.41 (d, J = 9.6 Hz, 1H), 6.76 (s, 2H), 7.06–7.10 (m, 1H), 7.14 (d, J = 2.2 Hz, 1H), 7.50 (d, J = 8.2 Hz, 1H), 7.70 (d, J = 9.3 Hz, 1H).

Synthesis of *N*-maleoyl-D-valine-2-nitrophenol ester (D-11b). The maleamic acid of D-valine **10** (500 mg, 2.54 mmol) was dissolved in 10 mL of thionyl chloride and heated at reflux until gas evolution had ceased. The

excess thionyl chloride was evaporated under reduced pressure. Carbon tetrachloride was added to the remaining material, and the resulting solution was evaporated under reduced pressure to insure complete removal of thionyl chloride. The resulting product was dissolved in 10 mL of CH_2Cl_2 and was slowly added to a stirred mixture of 2-nitrophenol (323 mg, 2.32 mmol) and triethylamine (0.64 mL, 4.64 mmol) in 10 mL of CH_2Cl_2 at 0 °C. The reaction mixture was allowed to warm to room temperature. After stirring an additional half hour at room temperature, the reaction mixture was diluted with 200 mL CH_2Cl_2, washed with brine, water, dried over Na_2SO_4 and concentrated in vacuo. The residue was flash chromatographed on silica gel (1:4 ethyl acetate/hexane) to afford the *N*-maleoyl-D-valine ester **D-11b**, 270 mg (37%). $[\alpha]_D = +25.5°$ (*c* 0.94, acetone); ^{1}H NMR (300 MHz, CD_3COCD_3) δ 0.93 (d, $J = 6.9$ Hz, 3H), 1.14 (d, $J = 6.9$ Hz, 3H), 2.68–2.75 (m, 1H), 4.72 (d, $J = 8.0$ Hz, 1H), 7.06 (s, 2H), 7.34–7.37 (m, 1H), 7.56–7.61 (m, 1H), 7.81–7.87 (m, 1H), 8.14–8.17 (m, 1H); ^{13}C NMR (300 MHz, CD_3COCD_3) δ 18.6, 20.2, 57.2, 125.3, 125.8, 127.6, 134.8, 135.3, 143.4, 166.5, 170.2.

Synthesis of *N*-maleoyl-D-valine coumarin ester (D-11c). The maleamic acid of D-valine **8** (500 mg, 2.54 mmol) was dissolved in 10 mL of thionyl chloride and heated at reflux until gas evolution had ceased. The excess thionyl chloride was evaporated under reduced pressure. Carbon tetrachloride was added to the remaining material, and the resulting solution was evaporated under reduced pressure to insure complete removal of thionyl chloride. The resulting product was dissolved in 10 mL of CH_2Cl_2 and was slowly added to a stirred mixture of 7-hydroxycoumarin (376 mg, 2.32 mmol) and triethylamine (0.64 mL, 4.64 mmol) in 10 mL of CH_2Cl_2 at 0 °C. The reaction mixture was allowed to warm to room temperature. After stirring an additional half hour at room temperature, the reaction mixture was diluted with 200 mL CH_2Cl_2, washed with brine, water, dried over Na_2SO_4 and concentrated in vacuo. The residue was flash chromatographed on silica gel (1:2 ethyl acetate/hexane) to afford the *N*-maleoyl-D-valine ester **D-11c**, 390 mg (49%). $[\alpha]_D = +85.2°$ (*c* 1.0, acetone); ^{1}H NMR (300 MHz, CD_3COCD_3) δ 0.93 (d, $J = 6.8$ Hz, 3H), 1.11 (d, $J = 6.8$ Hz, 3H), 2.60–2.64 (m, 1H), 4.79 (d, $J = 6.9$ Hz, 1H), 6.40 (d, $J = 9.6$ Hz, 1H), 7.05–7.10 (m, 4H), 7.72 (d, $J = 8.2$ Hz, 1H), 7.99 (d, $J = 9.6$ Hz, 1H); ^{13}C NMR (75 MHz, CD_3COCD_3) δ 19.0, 20.8, 57.3, 110.8, 116.8, 118.0, 119.1, 130.0, 135.5, 144.0, 153.8, 155.5, 160.1, 167.8, 171.2, 205.9, 206.2; HRMS (FAB) calcd for $C_{18}H_{16}NO_6$ $[M+H^+]$ 342.0978, found 342.0964.

Synthesis of *N*-maleoyl-L-valine coumarin ester (L-11c). This was prepared in 44% yield by the same method described for the D-valine derivative, **D-11c**. $[\alpha]_D = -83.5°$ (*c* 1.0, acetone).

General method for synthesis of the ester oligodeoxynucleotide conjugates 15 and 16. Oligodeoxynucleotide **14** (100 nmol) bearing a disulfide group[4] was reduced with TCEP (150 nmol) in 500 μL 0.1 M sodium phosphate buffer, pH 7.0, for 2 h at room temperature under argon. Maleimide ester (1 μmol in 50 μL acetonitrile) was added without elimination of the TCEP excess. The oligodeoxynucleotide conjugates were purified by reversed-phase HPLC on a Rainin Dynamax column (C-18, 5 μm, 4.6×250 mm) using two buffers: A (10% methanol and 90% 75 mM sodium phosphate buffer pH 7.0) and B (50% methanol and 50% 75 mM sodium phosphate buffer pH 7.0). A linear gradient was run from 0 to 100% B in 30 min, flow rate = 1.0 mL/min and the effluent was monitored by its absorbance at 260 nm. The desired fraction was collected, concentrated and desalted by using the same column, washed with excess doubly distilled water and eluted with 50:50 acetonitrile/water. The desalted fractions were combined and concentrated to dryness in vacuo. The product was analyzed by MALDI-TOF, **15a** calcd $(M-H^+)$ 2803.2, found 2802.9; **16c** calcd $(M-H^+)$ 2831.3, found 2832.6; **16c** calcd $(M-H^+)$ 2853.4, found 2852.6.

Kinetics of *p*-nitrophenol and 7-hydroxycoumarin release from the hairpin and three-component systems

For typical assays, phenol or coumarin oligodeoxynucleotide conjugates **15** or **16** and the imidazole hairpin **3a** or the complex **3b**/**4** were incubated in 10 mM sodium phosphate, pH 7.0, which contained 0.1 or 1.0 M NaCl. The reaction temperature was maintained at 20 °C, and the production of phenolate or 7-hydroxycoumarin was monitored by UV absorbance at 400 nm ($\varepsilon_{400} = 6.26\times10^3$ at pH 7) or by fluorescence ($\lambda_{Ex} = 355$ nm, $\lambda_{Em} = 452$ nm). Initial velocities of the reaction, obtained for each substrate concentration, were fitted to the Michaelis–Menten equation by a nonlinear least squares method using KaleidaGraph software. The inhibition constant K_I was determined in the presence of 25 μM 7 d(TCCTGTCA) in 10 mM sodium phosphate buffer pH 7.0 containing 1.0 M NaCl by the plotting $1/v$ versus $1/[S]$ and calculating K_I from the slope of the line according following equation:

$$\frac{1}{v} = \frac{1}{V_{max}} + \frac{K_M(1+\frac{[I]}{K_I})}{V_{max}} \times \frac{1}{[S]}$$

where v is the velocity of the reaction, V_{max} is the maximum velocity, K_M is the substrate concentration at half maximal reaction rate, [I] is the inhibitor concentration, and [S] is the substrate concentration.

Kinetics of *p*-nitrophenol and 7-hydroxycoumarin release by imidazole alone

For comparison purposes, the rate constant k_{Im} for the imidazole catalyzed hydrolysis of the various esters were determined in imidazole buffer at pH 7.0, 0.5 M NaCl at 20 °C as previously described.[42] The imidazole buffers were prepared in 0.5 M NaCl, and adjusted to pH 7 by addition of 1 M HCl. The hydrolysis reaction was followed by monitoring the absorbance of the phenolate

ion at 400 nm or the fluorescence emission of 7-hydroxycoumarin at 452 nm ($\lambda_{Ex} = 350$ nm) as a function of time. In a typical run, 5 μL of the ester (8 mM in acetonitrile for the phenyl esters and 200 μM in acetonitrile for the 7-hydroxycoumarin esters) were added to a cuvette containing 400 μL of imidazole buffer (0.004–0.6 M), capped and mixed by inverting several times. The pseudo first-order rate constant for each concentration of imidazole was obtained by linear least squares fitting of $\ln(A_\infty - A)$ or $\ln(F_\infty - F)$ versus time. The rate constants were then plotted against total imidazole concentration to get k_o, the first order rate constant for the uncatalyzed hydrolysis reaction, and k_{Im}, the second-order rate constant for catalysis by imidazole buffer.

Hydrolysis of esters in human serum

The hydrolysis of the coumarin esters **9c**, **11c**, **12c**, and **13c** was followed in a SPEX Fluoromax spectrofluorimeter at the following wavelengths: $\lambda_{Ex} = 350$ nm, $\lambda_{Em} = 452$ nm. In a typical run, 3 μL of coumarin ester solution (7 mM in acetonitrile) was added to 400 μL of Human serum, pH 8.3 (Innovative Research Inc.) in a cuvette. The cuvette was capped, inverted several times for thorough mixing, placed in a cell block and recording began. The appearance of 7-hydroxycoumarin was monitored at 452 nm at room temperature. The same procedure was followed for monitoring the hydrolysis of the *o*-nitrophenyl ester **11b** except that the solution was centrifuged in an Eppendorf centrifuge prior to making absorbance measurements at 400 nm.

Acknowledgements

This work was supported in part by NIH grant CA40463 and a Wheeler Fellowship for Z. Ma. The assistance of the Washington University High Resolution NMR Facility, funded in part through NIH Biomedical Research Support Shared Instrument Grants RR-02004, RR-05018, and RR-07155 is gratefully acknowledged, as is the Washington University Mass Spectrometry Resource, an NIH Research Resource (Grant No. P41RR0954).

References and Notes

1. Albert, A. *Selective Toxicity. The Physico-chemical Basis of Therapy*, 6th ed.; Chapman and Hall: London, 1979.
2. Drews, J. *Science* **2000**, *287*, 1960.
3. Gibbs, J. B. *Science* **2000**, *287*, 1969.
4. Denny, W. A. *Curr. Pharm. Des* **1996**, *2*, 281.
5. Sinhababu, A. K.; Thakker, D. R. *Adv. Drug Deliv. Rev.* **1996**, *19*, 241.
6. Melton, R.; Connors, T.; Knox, R. J. *S.T.P. Pharma Sci.* **1999**, *9*, 13.
7. Chari, R. V. J. *Adv. Drug Deliv. Rev.* **1998**, *31*, 89.
8. Sherwood, R. F. *Adv. Drug Deliv. Rev.* **1996**, *22*, 269.
9. Springer, C. J.; Niculescu-Duvaz, I. *Adv. Drug Deliv. Rev.* **1996**, *22*, 351.
10. Connors, T. A.; Knox, R. J. *Stem Cells (Dayton)* **1995**, *13*, 501.
11. Senter, P. D.; Svensson, H. P. *Adv. Drug Deliv. Rev.* **1996**, *22*, 341.
12. Dubowchik, G. M.; Walker, M. A. *Pharmacol. Ther.* **1999**, *83*, 67.
13. Ma, Z.; Taylor, J.-S. *Proc. Natl. Acad. Sci. U.S.A.* **2000**, *97*, 11159.
14. Golub, T. R.; Slonim, D. K.; Tamayo, P.; Huard, C.; Gaasenbeek, M.; Mesirov, J. P.; Coller, H.; Loh, M. L.; Downing, J. R.; Caligiuri, M. A.; Bloomfield, C. D.; Lander, E. S. *Science* **1999**, *286*, 531.
15. Gerhold, D.; Rushmore, T.; Caskey, C. T. *Trends Biochem. Sci.* **1999**, *24*, 168.
16. Antao, V. P.; Tinoco, I., Jr. *Nucleic Acids Res.* **1992**, *20*, 819.
17. Bender, M. L. *J. Am. Chem. Soc.* **1957**, *79*, 1652.
18. Bruice, T. C.; Schmir, G. L. *J. Am. Chem. Soc.* **1957**, *79*, 1663.
19. Bruice; Sturtevant, *J. Am. Chem. Soc.* **1959**, *81*, 2860.
20. Bender, M. L.; Turnquest, B. W. *J. Am. Chem. Soc.* **1957**, *79*, 1656.
21. Gesson, J. P.; Jacquesy, J. C.; Mondon, M.; Petit, P.; Renoux, B.; Andrianomenjanahary, S.; Dufat-Trinh Van, H.; Koch, M.; Michel, S.; Tillequin, F.; Florent, J. C.; Monneret, C.; Bosslet, K.; Czech, J.; Hoffmann, D. *Anti-C Drug Des.* **1994**, *9*, 409.
22. Lougerstay-Madec, R.; Florent, J.-C.; Monneret, C.; Nemati, F.; Poupon, M. F. *Anti-Cancer Drug Des.* **1998**, *13*, 995.
23. Madec-Lougerstay, R.; Florent, J.-C.; Monneret, C. *J. Chem. Soc., Perkin Trans. 1*, 1369.
24. Ueda, Y.; Matiskella, J. D.; Mikkilineni, A. B.; Farina, V.; Knipe, J. O.; Rose, W. C.; Casazza, A. M.; Vyas, D. M. *Bioorg. Med. Chem. Lett.* **1995**, *5*, 247.
25. Hovinen, J.; Guzaev, A.; Azhayeva, E.; Azhayev, A.; Lonnberg, H. *J. Org. Chem.* **1995**, *60*, 2205.
26. SantaLucia, J., Jr. *Proc. Natl. Acad. Sci. U.S.A.* **1998**, *95*, 1460.
27. Laurent, A.; Debart, F.; Lamb, N.; Rayner, B. *Bioconjugate Chem.* **1997**, *8*, 856.
28. SantaLucia, J., John.; Allawi, H. T.; Seneviratne, P. A., *Biochemistry* **1996**, *35*, 3555.
29. Arar, K.; Monsigny, M.; Mayer, R. *Tetrahedron Lett.* **1993**, *34*, 8087.
30. Frazier, K. A. US Patent 4,980,482, 1990.
31. Fersht, A. *Enzyme Structure and Mechanism*; W. H. Freeman: New York, 1985.
32. Bloomfield, V. A.; Crothers, D. M.; Inioco, I. *Nucleic Acids: Structures, Properties, and Functions*; University Science Books: Sausalito, CA, 1999.
33. Gelfand, C. A.; Plum, G. E.; Mielewczyk, S.; Remeta, D. P.; Breslauer, K. J. *Proc. Natl. Acad. Sci. U.S.A.* **1999**, *96*, 6113.
34. Peyret, N.; Seneviratne, P. A.; Allawi, H. T.; SantaLucia, J., Jr. *Biochemistry* **1999**, *38*, 3468.
35. Stoops, J. K.; Horgan, D. J.; Runnegar, M. T. C.; De Jersey, J.; Webb, E. C.; Zerner, B. *Biochemistry* **1969**, *8*, 2026.
36. Chakravarty, P. K.; Carl, P. L.; Weber, M. J.; Katzenellenbogen, J. A. *J. Med. Chem.* **1983**, *26*, 633.
37. Campbell, D. A.; Gong, B.; Kochersperger, L. M.; Yonkovich, S.; Gallop, M. A.; Schultz, P. G. *J. Am. Chem. Soc.* **1994**, *116*, 2165.
38. Miyazawa, T. *Amino Acids* **1999**, *16*, 191.
39. Milstien, J. B.; Fife, T. H. *J. Amer. Chem. Soc.* **1968**, *90*, 2164.
40. Fink, D. W.; Koehler, W. R. *Anal. Chem.* **1970**, *42*, 990.
41. Pollack, S. J.; Schultz, P. G. *J. Am. Chem. Soc.* **1989**, *111*, 1929.
42. Lombardo, A. *J. Chem. Educ.* **1982**, *59*, 887.